scientific reports

Check for updates

OPEN

A stochastic approach for co-evolution process of virus and human immune system

Qura Tul Ain[1,2], Jiahao Shen[2], Peng Xu[2], Xiaoli Qiang[3] & Zheng Kou[2]✉

Infectious diseases have long been a shaping force in human history, necessitating a comprehensive understanding of their dynamics. This study introduces a co-evolution model that integrates both epidemiological and evolutionary dynamics. Utilizing a system of differential equations, the model represents the interactions among susceptible, infected, and recovered populations for both ancestral and evolved viral strains. Methodologically rigorous, the model's existence and uniqueness have been verified, and it accommodates both deterministic and stochastic cases. A myriad of graphical techniques have been employed to elucidate the model's dynamics. Beyond its theoretical contributions, this model serves as a critical instrument for public health strategy, particularly predicting future outbreaks in scenarios where viral mutations compromise existing interventions.

Keywords Equilibrium, Extinction, Stability analysis, Immune system

Infectious diseases have shaped human history, leading to profound societal and cultural impacts. As our understanding of epidemiology has evolved, so too has the complexity of the models we use to predict and understand disease dynamics. The interplay between pathogens and hosts is a continuous arms race; while pathogens mutate to become more virulent or avoid host immunity, hosts evolve to develop improved resistance or immunity against these pathogens. This cyclical nature of adaptation and counter-adaptation (Fig. 1) has been a crucial element in the evolutionary history of many species, including humans.

In recent years, with the rise of diseases caused by rapidly mutating viruses, there is a heightened interest in understanding not just the dynamics of disease spread, but also how evolution plays a role in these dynamics. Traditional epidemiological models, such as the SIR (Susceptible-Infectious-Recovered) model, focus primarily on disease transmission without accounting for evolutionary changes in the virus or the host. In the landscape of infectious disease modeling, several pivotal works have laid the groundwork for comprehensive understanding. Authors in[1] discussed a mathematical model accounting for the dynamics of multiple SARS-CoV-2 strains focused on the impact of variants on pandemic trajectories and vaccine response. The study emphasizes the utility of the model in predicting variant rises and informing vaccination strategies.[2] took a generic approach to mathematical modeling of multi-strain pandemics, while[3] presented a model that focused on leveraging multiple strains with mutations in the context of COVID-19. Contributions from[4] incorporated vaccination dynamics into a two-strain model of COVID-19, whereas the work in[5] emphasized the diverse outcomes among COVID-19 patients. Study in[6] discussed the impact of reproduction numbers on multiwave spreading dynamics, while[7] focused on the interplay between innate and adaptive immune responses.[8] analyzed the host immunological response to adenovirus-based COVID-19 vaccines. Evidences from[9] brought forth a model assessing the level of cross-immunity between influenza strains.

A research develops a two-strain COVID-19 transmission model addressing the emergence of variants with different transmission dynamics and analyzing the impact of vaccination on one of the strains. It provides a theoretical framework with sufficient conditions for equilibrium stability, calculating the basic reproduction numbers and exploring scenarios for dominant strain establishment[10]. The competition between different SARS-CoV-2 variants in France using a mathematical model to estimate the impact of three variants on the spread of COVID-19, employing data from Geodes and a particle swarm optimization algorithm to estimate the basic reproduction number can be seen in[11]. A fractional model of two-strains covid disease was discussed by[12].

[1]School of Mathematics and Information Science, Guangzhou University, Guangzhou 510006, China. [2]Institute of Computing Science and Technology, Guangzhou University, Guangzhou 510006, China. [3]School of Computer Science and Cyber Engineering, Guangzhou University, Guangzhou 510006, China. ✉email: kouzheng@gzhu.edu.cn

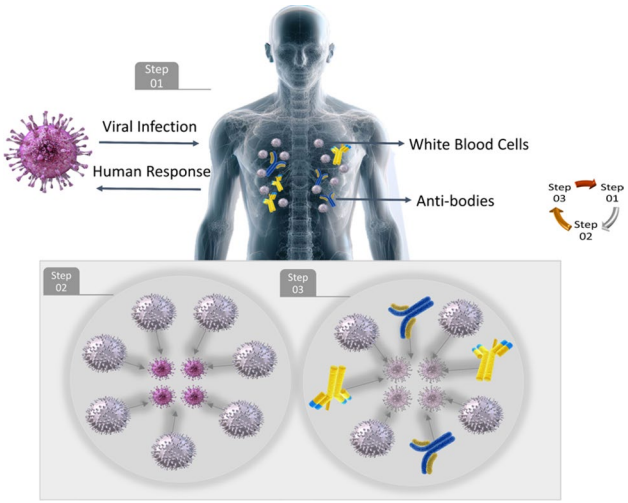

Figure 1. Virus and immune system's co-evolution process.

Collectively, these references provide a rich tapestry of insights into the evolving dynamics of infectious diseases. However, to truly grasp the progression and potential future trajectories of such diseases, one must consider the evolutionary dynamics in tandem with epidemiological ones.

Motivation

Our study advances the understanding of multiple infection dynamics, building on significant previous research in disease modeling. We resonate with and expand upon the work of researchers like those cited in[13,14], and[15], who explored transmission dynamics and sensitivity analysis using fractal-fractional differential operators. Our methodology also draws from[16,17], who developed fractional models for diseases such as malaria and typhoid fever, underscoring the critical role of analyzing multiple pathogens in epidemiological studies and the importance of understanding their reproduction numbers.

Furthermore, we recognize the impact of stochastic components in modeling diseases, as highlighted in[18]. The incorporation of time delays in stochastic epidemic models introduces complex system behaviors. The research in[19,20], and[21] demonstrates how mathematical and statistical approaches can be employed to tackle questions of stochasticity and stability in epidemic models. Additionally,[22]'s work on modeling COVID-19 with fractional order calculus emphasizes the effect of policy measures like isolation and vaccination on disease control, complementing our discussions on the efficacy of public health interventions.

Li and colleagues' contributions[23,24,25] shed light on the dynamic behavior of epidemic models, especially regarding bifurcations and chaotic phenomena, offering a valuable backdrop to our findings on oscillatory behaviors near endemic equilibrium.

Contribution

This work introduces a co-evolution model that seeks to capture this intricate balace between evolving viruses and the evolving human immune response. This model, built upon differential equations, represents the interaction dynamics of susceptible, infected, and recovered populations with both the original and evolved virus strains. By integrating evolutionary considerations into traditional epidemiological models, we aim to provide a more nuanced and comprehensive understanding of disease dynamics in the face of viral mutations and changing host immunities.

Novelty

Stochastic modeling plays a crucial role in epidemiology for several reasons. It allows researchers to account for the inherent randomness and variability in disease transmission among individuals and communities, reflecting the real-world unpredictability of outbreaks. This is vital for accurately simulating the spread of diseases and assessing potential outcomes under different scenarios. Stochastic models help in estimating the probabilities of different epidemiological events, enabling public health officials to make informed decisions regarding intervention strategies and resource allocation. Through stochastic modeling, epidemiologists can better understand the dynamics of infectious diseases, including the impact of factors like vaccination rates, population density, and social behaviors, thereby improving the effectiveness of disease control and prevention measures.

Beyond its theoretical significance, this model serves as a tool to guide public health interventions, and predict potential future outbreaks, especially in scenarios where rapid viral mutations might render existing treatments or vaccines less effective over time. In the subsequent sections, we will delve into the assumptions underlying the model, the mathematical formulations representing the co-evolution dynamics, and potential applications and implications of the findings derived from this model.

Model explanation

The model captures the interplay between human immunity and viral evolution. As the virus spreads, the human immune response evolves, leading to a changing transmission rate for the virus. The model can be used to analyze the impact of various interventions.

$$\begin{aligned}
\frac{d\check{S}_1}{dt} &= \mu - \beta_1 \check{S}_1 \check{I}_1 - \beta_2 \check{S}_1 \check{I}_2 + \rho \check{R} - \delta \check{S}_1,\\
\frac{d\check{S}_2}{dt} &= -\beta_2 \check{S}_2 \check{I}_2 - \beta_1 \check{S}_2 \check{I}_1 - \delta \check{S}_2,\\
\frac{d\check{I}_1}{dt} &= \beta_1 \check{S}_2 \check{I}_1 - \gamma \check{I}_1 - \sigma \check{I}_1 - \delta \check{I}_1,\\
\frac{d\check{I}_2}{dt} &= \beta_2 \check{S}_1 \check{I}_2 - \gamma \check{I}_2 - \sigma \check{I}_2 - \delta \check{I}_2,\\
\frac{d\check{R}}{dt} &= \gamma \check{I}_1 + \gamma \check{I}_2 - \rho \check{R} - \delta \check{R}.
\end{aligned} \tag{1}$$

with

$$\beta_1 = \beta_2 = \beta_0 \times \left(1 + \alpha \times r \times I \times \left(1 - \frac{I}{K}\right)\right).$$

- $\check{S}_1$ and $\check{S}_2$ represent two subpopulations of the host species that are susceptible to infection by the virus strains $\check{I}_1$ and $\check{I}_2$, respectively.
- $\check{R}$ represents the recovered individuals.
- β_1 and β_2 are the transmission rates of the two virus strains
- r influences the rate at which the transmission rates (β_1 and β_2) change in response to changes in the total number of infected individuals.
- The parameter r significantly influences the transmission rates β_1 and β_2 for the two virus strains. Specifically, the transmission rates are defined as $\beta_1 = \beta_2 = \beta_0 \times \left(1 + \alpha \times r \times I \times \left(1 - \frac{I}{K}\right)\right)$, indicating that the value of r directly affects how the total number of infected individuals I influences β_1 and β_2. An increase in r amplifies the effect of changes in I on the transmission rates, due to the term $\alpha \times r \times I \times \left(1 - \frac{I}{K}\right)$. Thus, r acts as a modulator of the transmission rates' sensitivity to the infected population size, playing a crucial role in the disease's spread dynamics within the host population.
- The parameter α plays a crucial role in the model, acting as a factor within the feedback mechanism that influences the transmission rates β_1 and β_2. Its primary function is to modulate the effect of the infected population size on the transmission rates, enabling the model to incorporate dynamic changes in transmission potential that occur as the prevalence of infection within the population changes. The model considers a moderate level of feedback, wherein increases in the infected population proportionally adjust the transmission rates, but not to an extreme degree. This adjustment is critical for accurately modeling the spread of infectious diseases, as it reflects the complex interactions between host behavior, population density, and pathogen transmissibility that can affect the rate at which an infection spreads through a community.
- δ represents the death rate, μ is birth rate.
- ρ represents the rate at which recovered individuals lose immunity and move back into the susceptible category.

This models a loss of immunity over time. This work took motivation from recent work on stochastic modeling and infectious diseases models as discussed by[26–32]. The stochastic model is given by

$$\begin{aligned}
d\check{S}_1(t) &= \left[\mu - \beta_1 \check{S}_1 \check{I}_1 - \beta_2 \check{S}_1 \check{I}_2 + \rho \check{R} - \delta \check{S}_1\right] dt + \sigma_1 \check{S}_1(t) d\mathfrak{D}_1(t),\\
d\check{S}_2(t) &= \left[-\beta_2 \check{S}_2 \check{I}_2 - \beta_1 \check{S}_2 \check{I}_1 - \delta \check{S}_2\right] dt + \sigma_2 \check{S}_2(t) d\mathfrak{D}_2(t),\\
d\check{I}_1(t) &= \left[\beta_1 \check{S}_2 \check{I}_1 - \gamma \check{I}_1 - \sigma \check{I}_1 - \delta \check{I}_1\right] dt + \sigma_3 \check{I}_1(t) d\mathfrak{D}_3(t),\\
d\check{I}_2(t) &= \left[\beta_2 \check{S}_1 \check{I}_2 - \gamma \check{I}_2 - \sigma \check{I}_2 - \delta \check{I}_2\right] dt + \sigma_4 \check{I}_2(t) d\mathfrak{D}_4(t),\\
d\check{R}(t) &= \left[\gamma \check{I}_1 + \gamma \check{I}_2 - \rho \check{R} - \delta \check{R}\right] dt + \sigma_5 \check{R}(t) d\mathfrak{D}_5(t).
\end{aligned} \tag{2}$$

The model includes several σ parameters representing variability and stochastic effects:

- σ_1: Represents the variability in the susceptible population $\check{S}_1$, which arise from fluctuating contact rates or changes in population behavior that affect exposure to the first virus strain.
- σ_2: Captures the randomness in the second susceptible population $\check{S}_2$, which is due to similar factors as σ_1, but with different underlying causes or magnitudes, given that S_2 represent a different risk group.
- σ_3: Reflects the random fluctuations in the number of individuals infected with the first virus strain $\check{I}_1$, due to variations in the disease's infectiousness, reporting rates, or response to treatment.
- σ_4: Pertains to the variability in the infection rate of the second virus strain $\check{I}_2$, which differ from σ_3 as the new strain has distinct characteristics, that is, higher transmissibility.

- σ_5: Represents stochastic factors affecting the recovered population $\breve{R}$, such as differential rates of loss of immunity or the impact of interventions that are not consistent across the entire population.

Each σ parameter is paired with a corresponding Brownian motion term, which mathematically represents the random 'noise' contributing to the fluctuations in each compartment over time. By including these stochastic terms, the model becomes a set of stochastic differential equations (SDEs), providing a more nuanced and realistic simulation of the epidemiological process, which can now capture both the average trends and the variability around those averages. The following assumptions underlie the model:

- Every parameter within the system is a nonnegative, positive real number.
- The transmission rate of the virus can change based on the proportion of the infected population.
- Immunity to one strain does not confer immunity to the evolved strain.

Qualitative analysis

Definition 1 A system of differential equations is said to be Lipschitz continuous with respect to a variable x if there exists a constant L such that for any state variables x and y in a domain D, then

$$||f(x) - f(y)|| \leq L||x - y||.$$

Lemma 1 *Consider two solutions,* $(\breve{S_1}, \breve{S_2}, \breve{I_1}, \breve{I_2}, \tilde{R})$ *and* $(\breve{S_1}', \breve{S_2}', \breve{I_1}', \breve{I_2}', \tilde{R}')$*, of the stochastic system. Then, for each equation in the system, the difference between the rates of change for the two solutions is bounded by a constant times the difference between the solutions.*

Proof Taking equation for $\breve{S_1}$,

$$\begin{aligned}
&\left|\left(\mu - \beta_1\breve{S_1}\breve{I_1} - \beta_2\breve{S_1}\breve{I_2} + \rho\tilde{R} - \delta\breve{S_1}\right)\right. \\
&\quad \left. - \left(\mu - \beta_1\breve{S_1}'\breve{I_1}' - \beta_2\breve{S_1}'\breve{I_2}' + \rho\tilde{R}' - \delta\breve{S_1}'\right)\right|, \\
&\leq \left|\beta_1(\breve{S_1}\breve{I_1} - \breve{S_1}'\breve{I_1}') + \beta_2(\breve{S_1}\breve{I_2} - \breve{S_1}'\breve{I_2}') + \rho(\tilde{R} - \tilde{R}') + \delta(\breve{S_1} - \breve{S_1}')\right|, \\
&\leq \beta_1(|\breve{S_1} - \breve{S_1}'| \cdot |\breve{I_1}| + |\breve{S_1}| \cdot |\breve{I_1} - \breve{I_1}'|) \\
&\quad + \beta_2(|\breve{S_1} - \breve{S_1}'| \cdot |\breve{I_2}| + |\breve{S_1}| \cdot |\breve{I_2} - \breve{I_2}'|) \\
&\quad + \rho|\tilde{R} - \tilde{R}'| + \delta|\breve{S_1} - \breve{S_1}'|.
\end{aligned}$$

We can set,

$$L = \beta_1\left(|\breve{I_1}| + |\breve{S_1}|\right) + \beta_2\left(|\breve{I_2}| + |\breve{S_1}|\right) + \rho + \delta.$$

as an upper bound.

Repeating this process for the other equations, we can identify similar constants for each one. The largest of these constants then serves as the Lipschitz constant L for the whole system. □

Definition 2 A system is considered bounded if, for all solutions $x(t)$ of the system and some positive constant M, the inequality $||x(t)|| \leq M$ holds for all t.

Theorem 1 *The stochastic system, given appropriate initial conditions, exhibits bounded behavior.*

Proof Consider the first equation for $\breve{S_1}$:

$$\frac{dS_1}{dt} = \mu - \beta_1\breve{S_1}\breve{I_1} - \beta_2\breve{S_1}\breve{I_2} + \rho\tilde{R} - \delta\breve{S_1} + \xi_1(t).$$

Given that populations cannot be negative, the loss terms ($\beta_1\breve{S_1}\breve{I_1}$, $\beta_2\breve{S_1}\breve{I_2}$, $\delta\breve{S_1}$) ensure that $\breve{S_1}$ does not grow unbounded. Therefore, the deterministic part of the system is bounded. □

Theorem 2 *Given boundedness and Lipschitz continuity, there exists a unique solution to the stochastic model for all time.*

Proof For a system of stochastic differential equations (SDEs) of the form:

$$dX(t) = f(X(t))dt + g(X(t))dW(t).$$

where $dW(t)$ represents the Wiener process, the existence and uniqueness of its solution is ensured if:

- The coefficients f and g are bounded.
- The system is Lipschitz continuous.

We've shown that the system is Lipschitz continuous and bounded. Hence, we conclude that there exists a unique solution to the SDEs of our stochastic model for all time. □

Equilibrium analysis

The variational matrix is obtained by linearizing the system of differential equations around the equilibrium. If we denote the equilibria as $(\breve{S_{1e}}, \breve{S_{2e}}, \breve{I_{1e}}, \breve{I_{2e}}, \tilde{R}_e)$, the variational matrix $\mathcal{V}$ at this equilibrium is given by the Jacobian:

$$\mathcal{V} = \begin{pmatrix} -\beta_1\breve{I_{1e}} - \beta_2\breve{I_{2e}} - \delta & -\beta_1\breve{S_{1e}} - \beta_2\breve{S_{1e}} & \mu - \beta_1\breve{S_{1e}} & \mu - \beta_2\breve{S_{1e}} & \rho \\ -\beta_2\breve{I_{2e}} - \beta_1\breve{I_{1e}} & -\beta_2\breve{S_{2e}} - \beta_1\breve{S_{2e}} & \beta_1\breve{S_{2e}} & \beta_2\breve{S_{2e}} & 0 \\ \beta_1\breve{S_{2e}} & \beta_1\breve{I_{1e}} & -\gamma - \sigma - \delta & 0 & 0 \\ \beta_2\breve{S_{1e}} & \beta_2\breve{I_{2e}} & 0 & -\gamma - \sigma - \delta & 0 \\ \gamma & \gamma & -\rho & -\rho & -\delta \end{pmatrix}.$$

$E_1(0, 0, 0, 0, 0)$

Given the variational matrix at the equilibrium $\mathfrak{E}_1(0, 0, 0, 0)$, we have $\breve{I_{1e}} = \breve{I_{2e}} = \breve{S_{1e}} = \breve{S_{2e}} = \breve{R_e} = 0$.

$$\mathcal{V} = \begin{pmatrix} -\delta & 0 & \mu & \mu & \rho \\ 0 & 0 & 0 & 0 & 0 \\ 0 & 0 & -\gamma - \sigma - \delta & 0 & 0 \\ 0 & 0 & 0 & -\gamma - \sigma - \delta & 0 \\ \gamma & \gamma & -\rho & -\rho & -\delta \end{pmatrix}.$$

The eigenvalues of the variational matrix $\mathcal{V}$ at the equilibrium point $\mathfrak{E}_1(0, 0, 0, 0, 0)$ are $-\delta$, 0, $-\gamma - \sigma - \delta$,$-\gamma - \sigma - \delta$,$-\delta$. Therefore, the equilibrium $\mathfrak{E}_1(0, 0, 0, 0, 0)$ is semi-stable based on the eigenvalues of the variational matrix.

Theorem 3 *The stability point $E_1(0, 0, 0, 0, 0)$ exhibits local asymptotic stability provided that $\delta > 0, \gamma + \sigma + \delta > 0$.*

$E_2(1, 0, 0, 0, 0)$

Given the equilibrium $\mathfrak{E}_1(1, 0, 0, 0, 0)$ where $\breve{I_{1e}} = 1, \breve{I_{2e}} = \breve{S_{1e}} = \breve{S_{2e}} = \breve{R_e} = 0$, substituting in the values for the equilibrium, we get,

$$\mathcal{V}_{\mathfrak{E}_1} = \begin{pmatrix} -\beta_1 - \delta & 0 & \mu & \mu & \rho \\ -\beta_1 & 0 & 0 & 0 & 0 \\ 0 & \beta_1 & -\gamma - \sigma - \delta & 0 & 0 \\ 0 & 0 & 0 & -\gamma - \sigma - \delta & 0 \\ \gamma & \gamma & -\rho & -\rho & -\delta \end{pmatrix}.$$

The eigenvalues are $-\beta_1 - \delta$,0,$-\gamma - \sigma - \delta$,$-\gamma - \sigma - \delta$,$-\delta$.

Theorem 4 *The stability point $E_2(1, 0, 0, 0, 0)$ exhibits local asymptotic stability provided that $\beta_1 + \delta > 0$, $\gamma + \sigma + \delta > 0, \delta > 0$.*

The remaining part of equilibrium analysis can be found in Appendix section 12.1.

Endemic equilibrium

The asymptotic solution relies heavily on the basic reproduction number R_0 of the disease, which is the expected number of cases directly generated by one case in a population where all individuals are susceptible to infection[33]. The presence of an endemic equilibrium depends on various factors, including the basic reproduction number R_0. The Jacobian matrix J of the system at the DFE (disease free equilibrium) is given by:

$$J = \begin{bmatrix} \mu - \delta & 0 & -\beta_1\breve{S_1} & -\beta_2\breve{S_1} & \rho \\ 0 & -\delta & -\beta_2\breve{S_2} & -\beta_1\breve{S_2} & 0 \\ 0 & 0 & -\gamma - \sigma - \delta & 0 & 0 \\ 0 & 0 & 0 & -\gamma - \sigma - \delta & 0 \\ 0 & 0 & \gamma & \gamma & -\rho - \delta \end{bmatrix}.$$

The next-generation matrix, K, is given by the product of two matrices, F and V^{-1}, For our system, the matrix F is

$$F = \begin{bmatrix} \beta_1\breve{S_2} & 0 \\ 0 & \beta_2\breve{S_1} \end{bmatrix}.$$

The matrix V is

$$V = \begin{bmatrix} \gamma+\sigma+\delta & 0 \\ 0 & \gamma+\sigma+\delta \end{bmatrix}.$$

The inverse is

$$V^{-1} = \begin{bmatrix} \frac{1}{\gamma+\sigma+\delta} & 0 \\ 0 & \frac{1}{\gamma+\sigma+\delta} \end{bmatrix}.$$

The next-generation matrix K is

$$K = F \times V^{-1} = \begin{bmatrix} \frac{\beta_1 \check{S}_2}{\gamma+\sigma+\delta} & 0 \\ 0 & \frac{\beta_2 \check{S}_1}{\gamma+\sigma+\delta} \end{bmatrix}.$$

Thus, R_0 is the maximum of the two diagonal entries.

$$R_0 = \max\left(\frac{\beta_1 \check{S}_2}{\gamma+\sigma+\delta}, \frac{\beta_2 \check{S}_1}{\gamma+\sigma+\delta}\right).$$

For R_{01} for $\check{I}_1$ is $\frac{\beta_2 \check{S}_1}{\gamma+\sigma+\delta}$, For R_{02} for $\check{I}_2$ is $\frac{\beta_1 \check{S}_2}{\gamma+\sigma+\delta}$. To determine the endemic equilibrium, we will evaluate the following basic reproduction numbers,

- $\mathbf{R}_{I_1}$ represents the mean count of recent infection cases attributed to I_1.
- $\mathbf{R}_{I_2}$ symbolizes the average count of new infection cases ascribed to I_2.

The system's critical parameter can be expressed as,

$$\mathbf{R}_0 = \max\left(\mathbf{R}_{I_1}, \mathbf{R}_{I_2}\right). \tag{3}$$

Beyond the equilibria highlighted earlier, the model's endemic equilibrium is realized when,

$$\min\left(\mathbf{R}_{I_1}, \mathbf{R}_{I_2}\right) > 1. \tag{4}$$

Theorem 5 *There exists a unique endemic equilibrium whenever* $R_0 > 1$.

Proof can be found in Appendix section 12.2.

Stochastic analysis

Suppose a probability domain represented as $(\Phi, \mathcal{G}, \mathbb{Q})$ containing a Wiener process (or Brownian motion) represented as $\mathcal{W} = \left\{\mathcal{W}_\pi, \mathcal{G}_\pi^{\mathcal{W}}, \pi > 0\right\}$. The associated filtration is given by $(\mathcal{G}_\pi, \pi > 0)$. Let

$$\mathrm{d}\mathbb{Z}(\pi) = \mathbf{y}(\pi, \mathbb{Z}(\pi))\mathrm{d}\mathcal{W}(\pi) + \mathbf{v}(\pi, \mathbb{Z}(\pi))\mathrm{d}\pi, \tag{5}$$

as the governing stochastic differential equation. The function $\mathbf{v}(\pi, \mathbb{Z}(\pi))$ maps from $[0, \infty) \times \mathbb{R}^e$ to $\mathbb{R}^e$. $\mathbf{y}(\pi, \mathbb{Z}(\pi))$ is considered to be an $p \times q$ matrix. In this scenario, both $\mathbf{y}$ and $\mathbf{v}$ satisfy Lipschitz conditions.

Let's introduce $\mathbf{K}$ as the differential operator for the system described in equation 5 ,

$$\mathbf{K} = \sum_{k=1}^{e} \mathbf{v}_k(\pi)\frac{\partial}{\partial w_k} + \frac{\partial}{\partial \pi} + \frac{1}{2}\sum_{k,l^*=1}^{e}\left[\mathbf{y}^T(w,\pi)\mathbf{y}(w,\pi)\right]_{kl}\frac{\partial^2}{\partial w_k \partial w_{l^*}}.$$

Applying operator $\mathbf{K}$ on a function Ψ, where $\Psi \in \mathbb{C}^{2,1}(\mathbb{R}^e \times [s_0, \infty); \mathbb{R}_+)$, we obtain,

$$\mathbf{K}\Psi(w,\pi) = \Psi_\pi(w,\pi) + \Psi_w(w,\pi)\mathbf{v}(w,\pi) + \frac{1}{2}\mathrm{trace}\left[f^T(w,\pi)\mathbf{y}(w,\pi)\right]. \tag{6}$$

Lemma 2 [34] *Suppose* $\mathbf{v} \in \mathbb{D}[[0,\infty] \times \Theta, (0,\infty)]$. *Our aim is to determine* κ_0 *and* $\kappa > 0$ *such that*,

$$\log \mathbf{v}(\mathrm{t}) \geq \kappa \mathrm{t} - \kappa_0 \int_0^{\mathrm{t}} \mathbf{v}(\mathrm{s})\mathrm{ds} + \mathbf{V}(\mathrm{t}) \text{ a.s..}$$

Given $\mathrm{t} \geq 0$ *and* $\mathbf{V} \in (\mathbb{D}[[0,\infty] \times \Theta, (0,\infty)])$ *satisfying* $\lim_{\mathrm{t}\to\infty} \frac{\mathbf{V}(\mathrm{t})}{\mathrm{t}} = 0$ *a.s., we obtain*,

$$\lim_{\mathrm{t}\to\infty} \langle \mathbf{v}(\mathrm{t}) \rangle \geq \frac{\kappa}{\kappa_0} \text{ a.s..}$$

Global existence

Theorem 6 The system has a bounded solution.
For the stochastic system with $\check{S}_1, \check{S}_2, \check{I}_1, \check{I}_2, R$, we define Ξ as,

$$\Xi = \left\{ (\check{S}_1(t), \check{S}_2(t), \check{I}_1(t), \check{I}_2(t), R(t)) \in \mathbb{R}_+^5 \middle| \sum_{i=1}^{5} X_i(t) \leq \frac{\nu}{\epsilon} \right\},$$

where X_i is the corresponding compartment. It remains to prove that Ξ adheres to the a.s., invariance principle.

Proof can be found in Appendix section 12.3.

Theorem 7 *Ξ adheres to the almost sure invariance principle for model* (1)*.*

Proof can be found in Appendix section 12.4.

Theorem 8 *For $\left(\check{S}_1(0), \check{S}_2(0), \check{I}_1(0), \check{I}_2(0), \check{R}(0)\right) \in \Xi$, the system* (1) *has unique and positive solution almost surely.*

Proof can be found in Appendix section 12.5.

Extinction

Lemma 3 *Consider $(\check{S}_1(t), \check{S}_2(t), \check{I}_1((t), \check{I}_2(t), \check{R}(t))$ as the solutions of the model* (1) *provided initial values $(\check{S}_1(0), \check{S}_2(0), \check{I}_1(0), \check{I}_2(0), \check{R}(0)) \in \Xi$, then*

$$\lim_{t\to\infty} \frac{\check{S}_1(t) + \check{S}_2(t) + \check{I}_1(t) + \check{I}_2(t) + \check{R}(t)}{t} = 0 \quad a.s,$$

$$\lim_{t\to\infty} \int_0^t \frac{\check{S}_1(r) d\mathfrak{D}_1(r)}{t} = 0 \text{ a.s},$$

$$\lim_{t\to\infty} \int_0^t \frac{\check{S}_2(r) d\mathfrak{D}_2(r)}{t} = 0 \text{ a.s},$$

$$\lim_{t\to\infty} \int_0^t \frac{\check{I}_1(r) d\mathfrak{D}_3(r)}{t} = 0 \text{ a.s},$$

$$\lim_{t\to\infty} \int_0^t \frac{\check{I}_2(r) d\mathfrak{D}_4(r)}{t} = 0 \text{ a.s.}$$

$$\lim_{t\to\infty} \int_0^t \frac{\check{R}(r) d\mathfrak{D}_4(r)}{t} = 0 \text{ a.s.}$$

We take

$$\mathbf{R}_1^s = \mathbf{R}_1 - \frac{1}{2} \frac{\varrho_3^2}{(b_1)},$$

$$\mathbf{R}_2^s = \mathbf{R}_2 - \frac{1}{2} \frac{\varrho_4^3}{(b_2)}.$$

Theorem 9 *Let $\check{S}_1(t), \check{S}_2(t), \check{I}_1(t), \check{I}_2(t), \check{R}(t)$ be the solution of the model with initial values*

$(\check{S}_1(0), \check{S}_2(0), \check{I}_1(0), \check{I}_2(0), \check{R}(0)) \in \Xi$. The disease go extinct almost surely, if $\mathbf{R}_1^s < 1$.

$$\lim_{t\to+\infty} \check{I}_1(t) = 0,$$

and

$$\lim_{t\to+\infty} \check{I}_2(t) = 0.$$

Proof See appendix section.

Analysis of the population dynamics

The following values in Table 1 has been used for numerical simulation. These values are based on theoretical studies and empirical findings[35–38]

Time series

The Euler-Maruyama method for a stochastic differential equation (SDE) of the form

$$dX_t = a(X_t, t)dt + b(X_t, t)dW_t,$$

is given by the following recursive formula,

$$X_{n+1} = X_n + a(X_n, t_n)\Delta t + b(X_n, t_n)\Delta W_n,$$

where $a(X_t, t)$ is the drift coefficient, $b(X_t, t)$ is the diffusion coefficient, and ΔW_n is the Wiener process increment approximated by $\sqrt{\Delta t} \cdot N(0, 1)$. The Euler-Maruyama approximation of the given stochastic model is,

$$\begin{aligned}
\breve{S}_1^{(n+1)} &= \breve{S}_1^{(n)} + \left[\mu - \beta_1 \breve{S}_1^{(n)} \breve{I}_1^{(n)} - \beta_2 \breve{S}_1^{(n)} \breve{I}_2^{(n)} + \rho \breve{R}^{(n)} - \delta \breve{S}_1^{(n)}\right] \Delta t + \sigma_1 \breve{S}_1^{(n)} \Delta \mathfrak{D}_1^{(n)}, \\
\breve{S}_2^{(n+1)} &= \breve{S}_2^{(n)} + \left[-\beta_2 \breve{S}_2^{(n)} \breve{I}_2^{(n)} - \beta_1 \breve{S}_2^{(n)} \breve{I}_1^{(n)} - \delta \breve{S}_2^{(n)}\right] \Delta t + \sigma_2 \breve{S}_2^{(n)} \Delta \mathfrak{D}_2^{(n)}, \\
\breve{I}_1^{(n+1)} &= \breve{I}_1^{(n)} + \left[\beta_1 \breve{S}_2^{(n)} \breve{I}_1^{(n)} - \gamma \breve{I}_1^{(n)} - \sigma \breve{I}_1^{(n)} - \delta \breve{I}_1^{(n)}\right] \Delta t + \sigma_3 \breve{I}_1^{(n)} \Delta \mathfrak{D}_3^{(n)}, \\
\breve{I}_2^{(n+1)} &= \breve{I}_2^{(n)} + \left[\beta_2 \breve{S}_1^{(n)} \breve{I}_2^{(n)} - \gamma \breve{I}_2^{(n)} - \sigma \breve{I}_2^{(n)} - \delta \breve{I}_2^{(n)}\right] \Delta t + \sigma_4 \breve{I}_2^{(n)} \Delta \mathfrak{D}_4^{(n)}, \\
\breve{R}^{(n+1)} &= \breve{R}^{(n)} + \left[\gamma \breve{I}_1^{(n)} + \gamma \breve{I}_2^{(n)} - \rho \breve{R}^{(n)} - \delta \breve{R}^{(n)}\right] \Delta t + \sigma_5 \breve{R}^{(n)} \Delta \mathfrak{D}_5^{(n)}.
\end{aligned}$$

- The susceptible populations, represented by $\breve{S}_1$ and $\breve{S}_2$, manifest a declining trend in Fig. 3. This reduction is indicative of the individuals transitioning to the infected categories, depleting the pool of individuals that can potentially be infected.
- The infected categories, represented by $\breve{I}_1$ and $\breve{I}_2$, show a typical infectious disease trajectory, an initial rise as the disease spreads through the susceptible population, a peak representing the maximum number of concurrent infections, and a subsequent decline as individuals recover or die.
- The $\breve{R}$ category, which denotes recovered individuals, exhibits an increasing trend, reflecting the accumulation of individuals who have gained immunity post-infection.

In Fig. 2, the deterministic lines depict an expected trajectory of populations, revealing trends of decline in susceptible classes, a peak in infections, and a rise in recoveries. In contrast, the stochastic lines mirror these general trends but with evident fluctuations, representing real-world variability due to unpredictable factors. Specifically, while susceptibles for both ancestral and evolved strains decrease over time, the evolved strain depletes the susceptible pool more rapidly. The number of infections shows varied dynamics, with the ancestral strain presenting a rapid rise and decline and the evolved strain maintaining a more consistent infection rate.

The recovered population steadily increases over time. The disparities between deterministic and stochastic representations underscore the importance of factoring in real-world randomness alongside average predictions in infectious disease modeling.

Parameter	Definition	Value	Source
$\breve{S}_{1_0}$	Initial Susceptible Population 1	0.475	Estimated
$\breve{S}_{2_0}$	Initial Susceptible Population 2	0.475	Estimated
$\breve{I}_{1_0}$	Initial Infected Population 1	0.01	Estimated
$\breve{I}_{2_0}$	Initial Infected Population 2	0.05	Estimated
$\breve{R}_0$	Initial Recovered Population	0.0	Estimated
β_0	Baseline Transmission Rate	0.5	Estimated
α	Modulation Factor for Transmission Rate	0.1	Estimated
r	Modulation Rate for β_1 and β_2	1.0	Estimated
K	Carrying Capacity for Infected Population	1.0	Estimated
γ	Recovery Rate	0.1	Estimated
μ	Birth Rate	0.02	Estimated
δ	Death Rate	0.01	Estimated
σ	Waning Immunity	0.01	Estimated
ρ	Reinfection rate	0.005	Estimated

Table 1. Initial and parametric values.

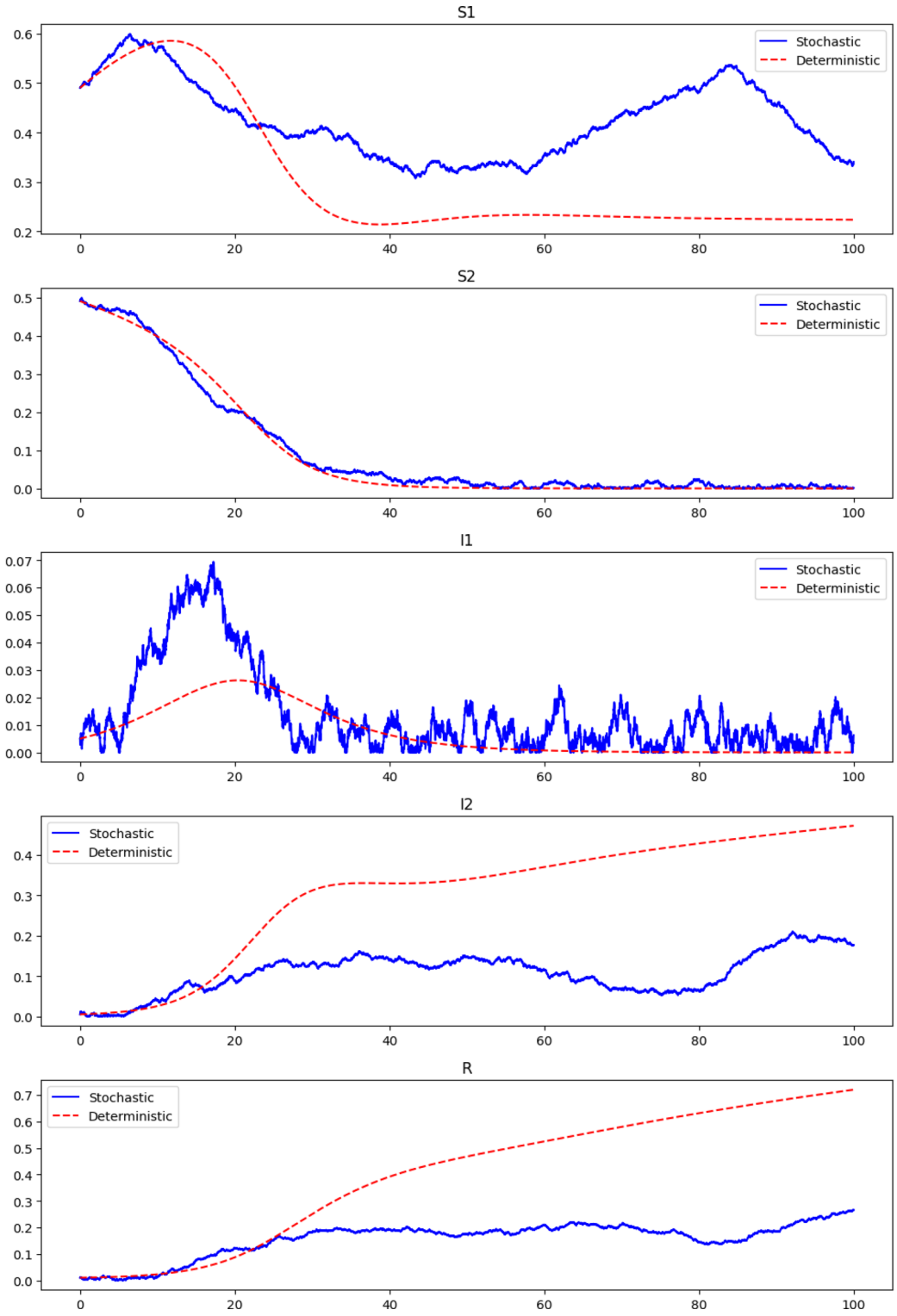

Figure 2. Stochastic VS deterministic time series.

$\check{I}_1$ is less virulent or less successful at sustaining its spread compared to $\check{I}_2$ given that $\check{I}_1$ dies out, while $\check{I}_2$ reaches a steady state. $\check{S}_1$ and $\check{S}_2$ both experience significant drops, but $\check{S}_1$ has a slight recovery, showing resistance in the population against $\check{I}_1$. The $\check{R}$ compartment's steady rise and plateau suggest that recovery is the primary outcome for infected individuals, which is a positive sign in terms of public health.

Parameter	Value	Source
$\check{S}_{1_0}$	0.475	Estimated
$\check{S}_{2_0}$	0.475	Estimated
$\check{I}_{1_0}$	0.01	Estimated
$\check{I}_{2_0}$	0.03	Estimated
$\check{R}_0$	0.0	[43]
β_0	0.6	[40]
α	0.2	[40]
r	1.2	Estimated
K	1.2	Estimated
γ	0.08	Estimated
μ	0.02	Estimated
δ	0.01	[36,39]
σ	0.02	Estimated
ρ	0.01	[36,39]

Table 2. Adjusted parametric values.

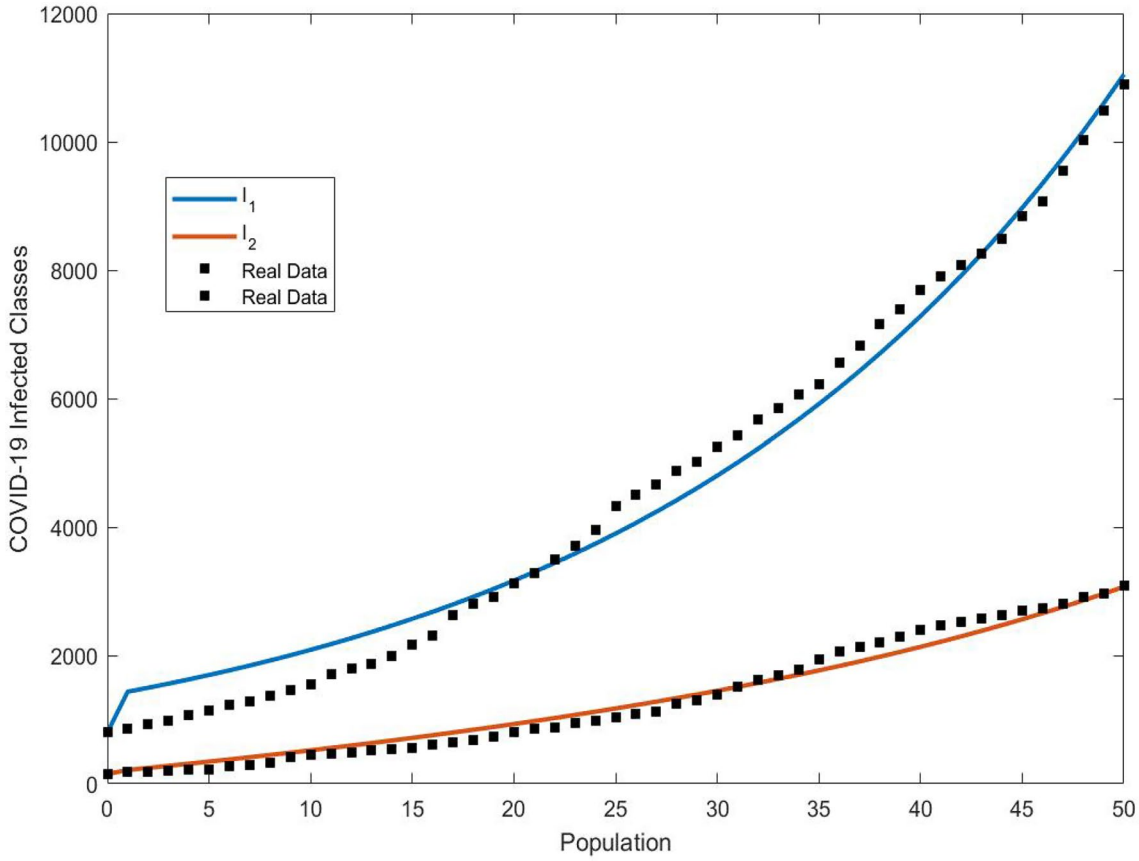

Figure 3. Real data analysis of COVID-19.

Real data

In Fig. 3, real data has been utilized to calibrate the model parameters for the alpha and beta variants of the SARS-CoV-2 virus given by Table 2, drawing on extensive datasets described in contemporary literature[11,35,39–43]. We have employed the nonlinear least square method for the estimation process. The Ordinary Least Square (OLS) solution was implemented to minimize the error terms as delineated in Eq. (7), and the related relative error was employed to assess the goodness of fit. Figure 3 illustrates the infected population as predicted by our proposed system with the real represented by stars.

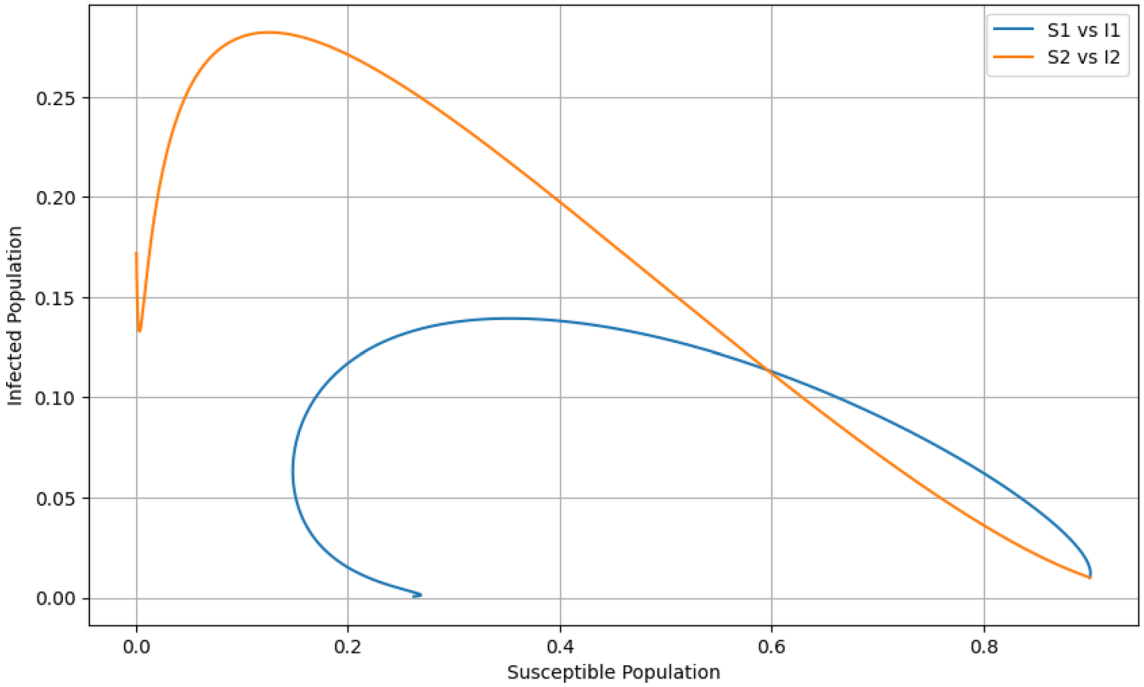

Figure 4. Phase plane plot.

$$\min\left\{\frac{\sum_{i=1}^{n}\left(I_i-\hat{I}_i\right)^2}{\sum_{i=1}^{n}I_i^2}\right\}. \tag{7}$$

Here the notion I_i is the reported cumulative infected cases and $\hat{I}_i$ is the cumulative infected cases obtained from simulating the model.

Phase plane plot

The trajectories in Fig. 4 reveal the cyclical nature of the interactions between susceptibility and infection, illuminating the ebb and flow of the epidemic. As susceptibles are depleted, the number of new infections decreases, leading to a decline in the infected populations. While $\check{I}_1$ have a cyclical pattern with $\check{S}_1$, indicating periods of outbreak and control, $\check{I}_2$ shows a more direct path to depletion of susceptibles, suggesting a more virulent or transmissible strain. This underlines the importance of strain-specific public health interventions.

Time series with moving average

While the raw data for $\check{I}_1$ and $\check{I}_2$ captures the actual number of infections, the moving average smoothens out short-term fluctuations, thereby highlighting broader trends. Both the actual infection data and the moving average exhibit a prominent peak, representing the height of the epidemic before a decline sets in. This underscores the transient nature of outbreaks and the eventual return to equilibrium as shown by Fig. 5.

Quiver plot

The quiver plot in Fig. 6 suggests complex interactions between the $\check{I}_1$ and $\check{I}_2$ strains. The arrows elucidate the direction and magnitude of change, providing a snapshot of the evolution in infection rates. The looping trajectory show oscillations in the infected populations, suggesting periodic outbreaks or potential for repeated waves of infections. This cyclic pattern arises from various factors, such as loss of immunity, seasonal variations, or reintroduction of infections.

Population distribution

This bar graph gives an overview of the distribution of different populations at a specific time, $t = 100$ in Fig. 7. By this time, a significant portion of the initial susceptible population have transitioned to the recovered category. The number of infected individuals ($\check{I}_1$ and $\check{I}_2$) is notably less than the susceptible and recovered groups, indicating that the epidemic is waning.

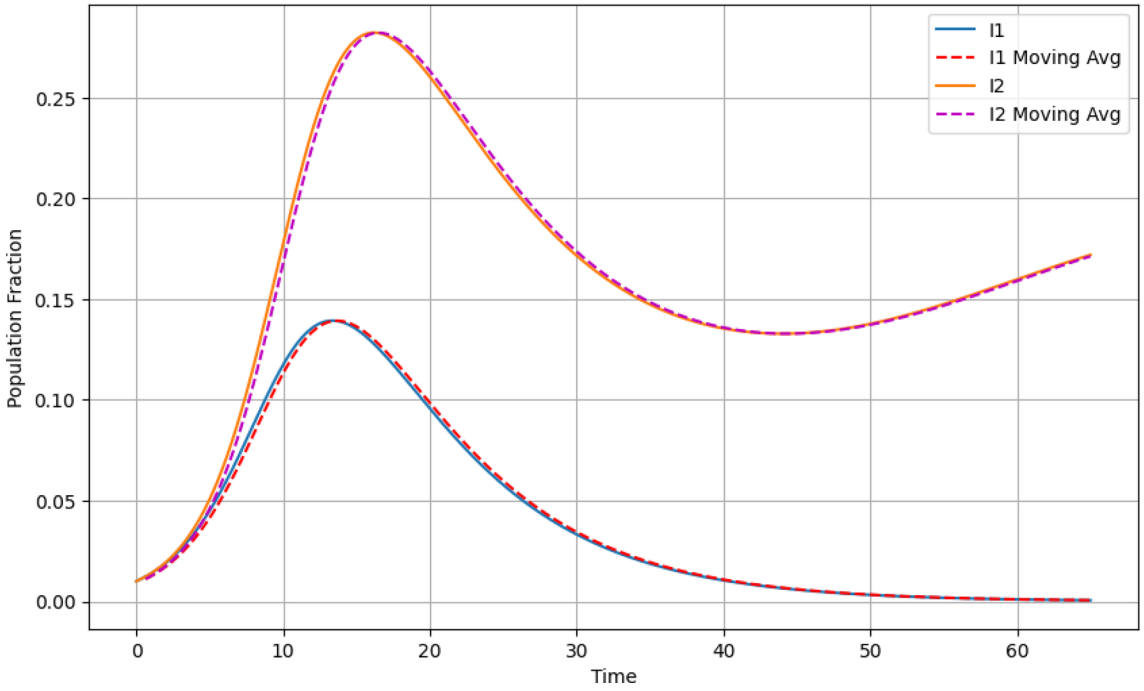

Figure 5. Time series with moving average.

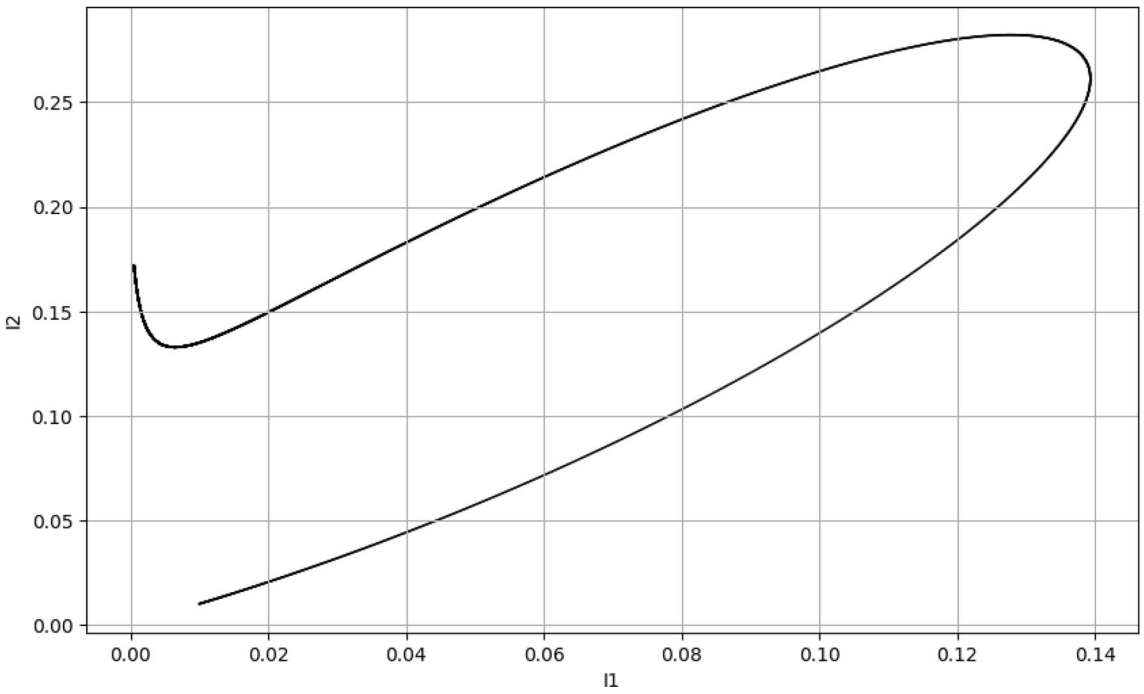

Figure 6. Quiver plot.

Conclusion

The introduced epidemiological model represents a significant enhancement in the mathematical study of infectious diseases, especially those with multiple circulating strains such as SARS-CoV-2. Authenticated by real data analysis, the model's equations provide a precise depiction of the disease dynamics, offering authenticity and bolstering its credibility within the scientific community.

The analysis of $\check{I}_1$ and $\check{I}_2$ through this model showcases a comprehensive mathematical characterization of the spread and potential control of multiple viral strains. The incorporation of empirical data not only underscores the model's accuracy but also fortifies its predictive capacity regarding disease progression and potential

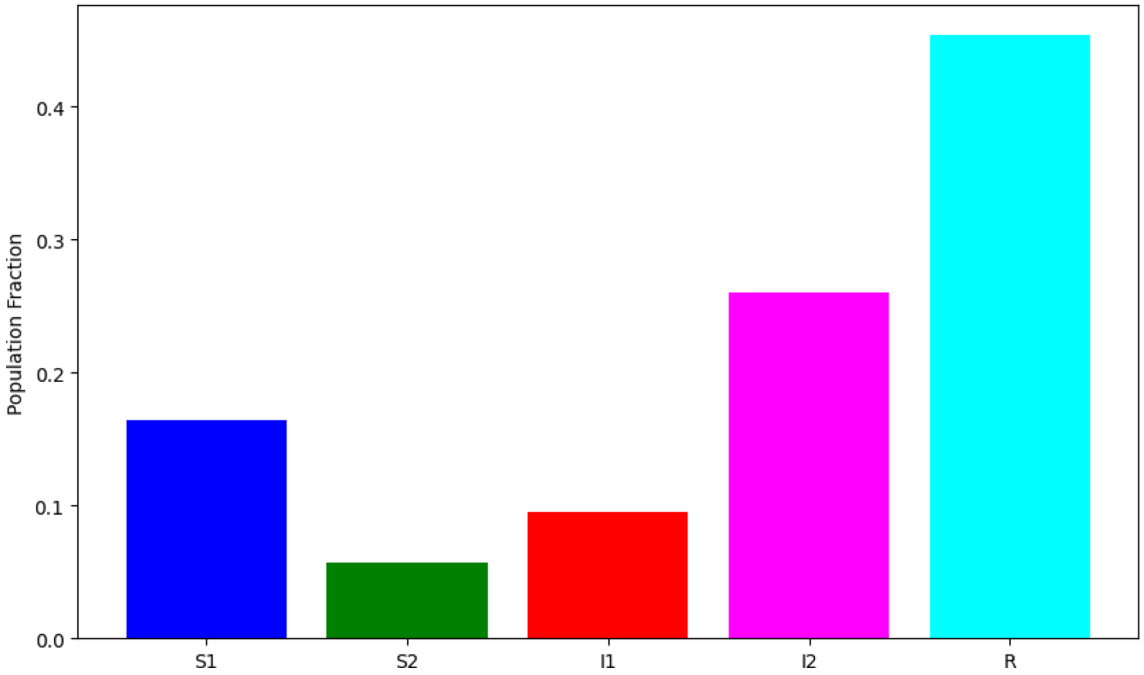

Figure 7. Population distribution at t = 100.

extinction scenarios. The model's robustness is affirmed through rigorous exploration of disease extinction conditions, laying a foundation for understanding the critical thresholds that govern the eradication of the disease.

The research by[10] models COVID-19's transmission with a focus on variant dynamics and vaccine impact, while[11] assesses the influence of variants in France using optimization for parameter estimation. The study in[12] introduces a fractional model for two COVID-19 strains, and[1] explores the impact of multiple strains on pandemic trajectories and vaccine efficacy. These studies contribute valuable insights into pandemic modeling; however, our work extends these efforts by offering a more intricate examination of disease dynamics, specially;

- Integrates a wider range of epidemiological and evolutionary dynamics.
- Provides a deeper analytical approach including a comprehensive equilibrium analysis, and disease extinction conditions.
- Offers a more detailed exploration of both deterministic and stochastic scenarios.
- Utilizes advanced graphical techniques for a clearer understanding of disease progression.
- Addresses practical applications for real-world outbreaks, especially in the context of evolving viral strains impacting public health measures.

Remarks and future recommendations

Our in-depth examination of the co-evolution model of host and human immune response highlights the intricate dynamics between infectious strains $\check{I}_1$ and $\check{I}_2$. The stark differences in the trajectories of these strains underscore the complex challenges posed in managing multi-strain infectious diseases. While our model offers a comprehensive understanding, the continually evolving nature of infectious diseases calls for adaptive strategies and persistent refinement in modeling approaches.

For future studies, it is recommended to incorporate factors like varying mutation rates, potential cross-immunity effects, and the impact of external interventions such as vaccination campaigns. Additionally, integrating real-world data can augment the model's predictive accuracy. As global communities grapple with the multifaceted challenges posed by infectious diseases, models such as ours serve as foundational tools, and their continuous refinement remains pivotal for informed public health decision-making.

Data availibility

All data generated or analysed during this study are included in this published article.

Received: 25 November 2023; Accepted: 29 April 2024
Published online: 06 May 2024

References

1. Yagan, O. *et al.* Modeling and analysis of the spread of COVID-19 under a multiple-strain model with mutations. *Harvard Data Sci. Rev.* **2021**, 4 (2021).
2. Lazebnik, T. & Bunimovich-Mendrazitsky, S. Generic approach for mathematical model of multi-strain pandemics. *PLoS ONE* **17**(4), e0260683 (2022).

3. Sridhar, A. *et al.* Leveraging a multiple-strain model with mutations in analyzing the spread of COVID-19. In *ICASSP 2021-2021 IEEE International Conference on Acoustics, Speech and Signal Processing (ICASSP)* 8163-8167 (IEEE, 2021).
4. de Le, U. A. P., Avila-Vales, E. & Huang, K. L. Modeling COVID-19 dynamic using a two-strain model with vaccination. *Chaos Soliton. Fract.* **157**, 111927 (2022).
5. Sahoo, S., Jhunjhunwala, S. & Jolly, M. K. The good, the bad and the ugly: A mathematical model investigates the differing outcomes among CoVID-19 patients. *J. Indian Inst. Sci.* **100**, 673–681 (2020).
6. Shayak, B., Sharma, M. M., Gaur, M. & Mishra, A. K. Impact of reproduction number on the multiwave spreading dynamics of COVID-19 with temporary immunity: A mathematical model. *Int. J. Infect. Dis.* **104**, 649–654 (2021).
7. Du, S. Q. & Yuan, W. Mathematical modeling of interaction between innate and adaptive immune responses in COVID-19 and implications for viral pathogenesis. *J. Med. Virol.* **92**(9), 1615–1628 (2020).
8. Farhang-Sardroodi, S. *et al.* Analysis of host immunological response of adenovirus-based COVID-19 vaccines. *Vaccines* **9**(8), 861 (2021).
9. Asatryan, M. N. *et al.* Mathematical model for assessing the level of cross-immunity between strains of influenza virus subtype H 3 N 2. *Probl. Virol.* **68**(3), 252–264 (2023).
10. Tchoumi, S. Y., Rwezaura, H. & Tchuenche, J. M. Dynamic of a two-strain COVID-19 model with vaccination. *Results Phys.* **39**, 105777 (2022).
11. Massard, M., Eftimie, R., Perasso, A. & Saussereau, B. A multi-strain epidemic model for COVID-19 with infected and asymptomatic cases: Application to French data. *J. Theor. Biol.* **545**, 111117 (2022).
12. Fatmawati, Y. E., Alfiniyah, C., Juga, M. L. & Chukwu, C. W. On the modeling of COVID-19 transmission dynamics with two strains: Insight through caputo fractional derivative. *Fract. Fract.* **6**(7), 346 (2022).
13. Ahmad, Z., Bonanomi, G., di Serafino, D. & Giannino, F. Transmission dynamics and sensitivity analysis of pine wilt disease with asymptomatic carriers via fractal-fractional differential operator of Mittag-Leffler kernel. *Appl. Numer. Math.* **185**, 446–465 (2023).
14. Malik, A. *et al.* Sensitivity analysis of COVID-19 with quarantine and vaccination: A fractal-fractional model. *Alex. Eng. J.* **61**(11), 8859–8874 (2022).
15. Ahmad, Z. *et al.* A global report on the dynamics of COVID-19 with quarantine and hospitalization: A fractional order model with non-local kernel. *Comput. Biol. Chem.* **98**, 107645 (2022).
16. Sinan, M. *et al.* Fractional mathematical modeling of malaria disease with treatment & insecticides. *Results Phys.* **34**, 105220 (2022).
17. Sinan, M. *et al.* Fractional order mathematical modeling of typhoid fever disease. *Results Phys.* **32**, 105044 (2022).
18. Wang, Y., Abdeljawad, T. & Din, A. Modeling the dynamics of stochastic norovirus epidemic model with time delay. *Fractals* **30**(05), 2240150 (2022).
19. Khan, F. M. & Khan, Z. U. Numerical analysis of fractional order drinking mathematical model. *J. Math. Tech. Model.* **1**(1), 11–24 (2024).
20. Khan, W. A., Zarin, R., Zeb, A., Khan, Y. & Khan, A. Navigating food allergy dynamics via a novel fractional mathematical model for antacid-induced allergies. *J. Math. Tech. Model.* **1**(1), 25–51 (2024).
21. Ain, Q. T. Nonlinear stochastic cholera epidemic model under the influence of noise. *J. Math. Tech. Model.* **1**(1), 52–74 (2024).
22. Sadek, L. *et al.* Fractional order modeling of predicting covid-19 with isolation and vaccination strategies in morocco. *CMES-Comput. Model. Eng. Sci* **136**, 1931–1950 (2023).
23. Jiang, X. *et al.* Bifurcation, chaos, and circuit realisation of a new four-dimensional memristor system. *Int. J. Nonlinear Sci. Numer. Simul.* **202**, 896 (2022).
24. Li, B., Eskandari, Z. & Avazzadeh, Z. Strong resonance bifurcations for a discrete-time prey-predator model. *J. Appl. Math. Comput.* **2023**, 1–18 (2023).
25. Li, B., Eskandari, Z. & Avazzadeh, Z. Dynamical behaviors of an SIR epidemic model with discrete time. *Fract. Fract.* **6**(11), 659 (2022).
26. Hedberg, P. *et al.* Bacterial co-infections in community-acquired pneumonia caused by SARS-CoV-2, influenza virus and respiratory syncytial virus. *BMC Infect. Dis.* **22**(1), 1–11 (2022).
27. Bhowmick, S., Sokolov, I. M. & Lentz, H. H. Decoding the double trouble: A mathematical modelling of co-infection dynamics of SARS-CoV-2 and influenza-like illness. *Biosystems* **2023**, 104827 (2023).
28. Wu, X., Gao, D., Song, Z. & Wu, J. Modelling *Trypanosoma cruzi-Trypanosoma rangeli* co-infection and pathogenic effect on Chagas disease spread. *Discrete Contin. Dyn. Syst.-B* **28**(2), 1024–1045 (2023).
29. Elaiw, A. M., Shflot, A. S. & Hobiny, A. D. Stability analysis of SARS-CoV-2/HTLV-I coinfection dynamics model. *AIMS Math.* **8**(3), 6136–6166 (2023).
30. Ojo, M. M., Peter, O. J., Goufo, E. F. D. & Nisar, K. S. A mathematical model for the co-dynamics of COVID-19 and tuberculosis. *Math. Comput. Simul.* **2023**, 114 (2023).
31. Din, A., Li, Y. & Omame, A. A stochastic stability analysis of an HBV-COVID-19 co-infection model in resource limitation settings. *Waves Random Complex Media* **2022**, 1–33 (2022).
32. Din, A., Khan, A. & Sabbar, Y. Long-term bifurcation and stochastic optimal control of a triple-delayed Ebola virus model with vaccination and quarantine strategies. *Fract. Fract.* **6**(10), 578 (2022).
33. Lazebnik, T. Computational applications of extended SIR models: A review focused on airborne pandemics. *Ecol. Model.* **483**, 110422 (2023).
34. Ain, Q. T. & Wang, J. A stochastic analysis of co-infection model in a finite carrying capacity population. *Int. J. Biomath.* **2023**, 2350083 (2023).
35. Lazebnik, T., Bunimovich-Mendrazitsky, S. & Shaikhet, L. Novel method to analytically obtain the asymptotic stable equilibria states of extended SIR-type epidemiological models. *Symmetry* **13**(7), 1120 (2021).
36. Özköse, F. Long-term side effects: A mathematical modeling of COVID-19 and stroke with real data. *Fract. Fract.* **7**(10), 719 (2023).
37. Edouard, M. *et al.* Coronavirus Pandemic (COVID-19). OurWorldInData.org. Retrieved from: 'https://ourworldindata.org/coronavirus' [Online Resource] (2020).
38. Yavuz, M., Cosar, F. & Ö., Günay, F., & Özdemir, F. N. A new mathematical modeling of the COVID-19 pandemic including the vaccination campaign. *Open J. Model. Simula.***9**(3), 299–321 (2021).
39. Tamilalagan, P., Krithika, B., Manivannan, P. & Karthiga, S. Is reinfection negligible effect in COVID-19? A mathematical study on the effects of reinfection in COVID-19. *Math. Methods Appl. Sci.* **46**(18), 19115–19134 (2023).
40. Ghosh, S. K. & Ghosh, S. A mathematical model for COVID-19 considering waning immunity, vaccination and control measures. *Sci. Rep.* **13**(1), 3610 (2023).
41. Dutta, A. COVID-19 waves: Variant dynamics and control. *Sci. Rep.* **12**(1), 9332 (2022).
42. Arruda, E. F., Das, S. S., Dias, C. M. & Pastore, D. H. Modelling and optimal control of multi strain epidemics, with application to COVID-19. *PLoS ONE* **16**(9), e0257512 (2021).
43. Mandal, M. *et al.* A model based study on the dynamics of COVID-19: Prediction and control. *Chaos Soliton. Fract.* **136**, 109889 (2020).

Acknowledgements
This work was supported by the National Natural Science Foundation of China (62172114, 61972109), the Natural Science Foundation of Guangdong Province of China (2022A1515011468) and the Fundings by Science and Technology Projects in Guangzhou(202201020237, SL2022A03J01035).

Author contributions
Q: Conceptualization, Methodology, Software, Writing - Original Draft Preparation. J: Visualization, Investigation. P: Formal Analysis, Validation. X: Resources, Supervision. Z(Corresponding Author): Project Administration, Funding Acquisition, Writing - Review & Editing. All authors reviewed the manuscript.

Competing interests
The authors declare no competing interests.

Additional information
Supplementary Information The online version contains supplementary material available at https://doi.org/10.1038/s41598-024-60911-z.

Correspondence and requests for materials should be addressed to Z.K.

Reprints and permissions information is available at www.nature.com/reprints.

Publisher's note Springer Nature remains neutral with regard to jurisdictional claims in published maps and institutional affiliations.